An Improved Double Vaseline Gap Voltage Clamp to Study Electroporated Skeletal Muscle Fibers

Wei Chen and Raphael C. Lee
Department of Surgery and Department of Organismal Biology and Anatomy, The University of Chicago, Chicago, Illinois 60637 USA

ABSTRACT An improved voltage clamp with a double vaseline gap chamber was designed to study electroporated skeletal muscle fibers. The new clamp eliminated spike overshock of membrane potential when applying step stimulation occurring in the traditional configuration. It allowed greater consistency in membrane potential distribution. After the intracellular resistances of the fiber segment at the vaseline gap area were compensated, it was possible to change membrane potential more quickly. Using this technique, strong electrical pulses used to mimic the situation of electrical shock can be delivered to the cell membrane by voltage clamp. Transmembrane currents of skeletal muscle cell were simultaneously measured during a high pulsed shock and resolved into different components. Distinct transient changes of the transmembrane current, involving the time courses of the formation of electroporation and their recovery time constants, can be recorded. Because of more even membrane potential distribution and faster response to pulsed membrane potential change, this technique is also suitable for membrane study under physiological conditions.

INTRODUCTION

Electroporation occurs when a strong electric field disrupts cell membrane structural integrity and results in the formation of transmembrace pores or defects (Tsong, 1991). One consequence of electroporation is a dramatic increase in the solute permeability and electrical conductivity of the cell membrane and the exchange of contents between the cell and its extracellular environment. Several investigators have applied electrical pulses to induce electropores in cell membranes to facilitate the uptake or discharge of a variety of molecules in living cells (Zimmermann et al., 1980; Wong and Neumann, 1982; Winegar et al., 1989; Chang et al., 1991). In general, relatively small, non-excitable cells have been used for this research.

Recently, electroporation was postulated to be an important mechanism of tissue damage in electrical trauma (Lee, 1990). There is growing interest in determining the factors that govern the process of electroporation, and, in particular, whether the process results in transient or stable poration. Attempts have also been made to identify chemical agents that will induce sealing of electrically mediated pores and help to restore membrane stability (Lee et al., 1992).

When a cell is exposed in an electrical field, the magnitude of transmembrane potential is proportional to the applied external electric field multiplied by the effective electrical dimensions of the whole cell (Cole, 1972). The equivalent intensity of the electrical field within the cell membrane induced by an applied external electric field is thus amplified by the ratio of cell dimension, L_{cell}, to the membrane thickness, d,

$$E_{equiva} \propto E_{ext}L_{cell}/2d. \quad (1)$$

For skeletal muscle and nerve fibers, if the external electrical field is parallel to the axis of the fiber, L_{cell} is the length of the cell, and if perpendicular to the fiber, L_{cell} is the diameter of the cell. Excitable cells, such as skeletal muscle and nerve cells, are relatively large, and the ratio of the size of a cell to the thickness of its membrane is on the order of 1000 or more. Because cell membranes of large cells tolerate the most voltage drop and sustain the most damage during electrical shock, studies of electroporation in electric trauma have, in general, focused on skeletal muscle and nerve fibers (Lee, 1990).

The kinetics of electroporation involve the initial molecular reorganization of the cell membrane and the secondary effect, pore or defect formation, processes that occur from within nanoseconds to subseconds (Tsong, 1991). The techniques used for monitoring these cellular responses to electrical shock must be fast as well as accurate, both during and after the shock. Experimental techniques used to study electroporation on skeletal muscle cell membranes have included morphological investigation using an electron microscope with freeze fracture (Chang and Reese, 1990) and permeability studies employing fluorescent dye (Lee et al., 1992, Chen et al., 1992). Tsong and colleagues measured the conductivity of the erythrocyte suspension to compare membrane electroporation and the field-induced effects on Na^+/K^+ ATPase (Teissie and Tsong, 1980; Serpersu and Tsong, 1983). All of these methods involve measurements taken after the electrical shock has occurred and have time resolution on the order of 10^{-1} s or less. An alternative method permitting higher time resolution uses a fluorescent voltage-sensitive dye to monitor membrane potential. Kinosita and co-workers (Hibino et al., 1991) have described a sub-microsecond measurement capability in studies of

Received for publication 12 April 1993 and in final form 14 December 1993.
Address reprint requests to Dr. Wei Chen, The University of Chicago, Section of Plastic and Reconstructive Surgery, 5841 South Maryland Avenue, Chicago, IL 60637.

0006-3495/94/03/700/10 $2.00

electroporation in a sea urchin egg. However, the disadvantage of their approach is that the total conductance of a cell membrane cannot be monitored at the onset of the shock and cannot be resolved into its components. Direct measurements of both membrane potential and transmembrane current require more refined techniques such as "charge injection" or "charge relaxation" and voltage clamp.

The charge injection/relaxation method permits a time resolution for transmembrane current in a nanosecond range (Benz and Zimmermann, 1980, 1981; Chernomordik et al., 1983). A cell membrane is charged with high-voltage current and then discharged. The rate of discharging curve depends on the membrane's capacitance and conductance. There is a very fast response time, but the injection/relaxation method can only monitor the transmembrane current of the cells immediately after, not during, the electrical charging. Another problem is that during the recording of the transmembrane current, the membrane potential decays exponentially and both transmembrane current and membrane potential vary during the measurement, making it difficult to calculate membrane conductance.

Voltage clamp techniques involve clamping a constant voltage across the cell membrane and simultaneously measuring the transmembrane current. The capability of monitoring changes in transmembrane current during the electrical shock makes it possible to calculate changes in membrane conductance directly and resolve it into different components. The voltage clamp employs a feedback circuit to adjust the compliance source to constrain the transmembrane potential as a constant, despite any changes in the cell membrane. This constant voltage drop on a cell membrane is difficult to achieve using external electrodes to provide shock electrical field because of the characteristic change of the cell membrane. The voltage clamp method has been used to study electroporation in artificial lipid bilayer preparations (Abidor et al., 1979; Chernomordik et al., 1987; Glaser et al., 1988), but it is not generally used with live cells (O'Neill and Tung, 1991). One difficulty is that the high internal resistance of microelectrodes limits the amount of transmembrane current, while large currents are required to damage the cell membrane.

This paper introduces an improved technique combining use of a cut skeletal muscle fiber in a double vaseline gap chamber with a voltage clamp to study electroporation. Using this new technique, we can keep the resistance of the voltage-applying electric circuit (not including the membrane itself) within a few thousand ohms, that is, several orders of magnitude lower than when microelectrodes are used. This new method allows us to apply a membrane potential change more quickly. Furthermore, this method makes it possible to shock cell membrane more evenly than the traditional method. Therefore, the advantage of the method we designed here is that we can deliver strong electrical shock pulses to cell membrane using voltage clamp and simultaneously record changes in the transmembrane current during the electric shock.

MATERIALS AND METHODS

Muscle and single fiber preparation

Semitendinous muscle fibers were obtained from English spice frogs, *Rana temporaria*. The animals were pseudo-hibernated in a cold-room at 4°C and then killed by instantaneous decapitation and pithing following a protocol approved by the University Institutional Animal Care and Use Committee. The protocol for dissection of single muscle fiber followed the procedure used by other investigators (Kovacs et al., 1983; Irving et al., 1987; Chen and Hui, 1991). Briefly, the pithed frog is pinned in a wax-filled Petri dish. A single, semitendinous muscle is dissected from its surrounding tissue and placed in a Petri dish filled with a concentrated potassium relaxing solution. This treatment is necessary to depolarize the muscle fiber and prevent a cell from contracting during dissection and experimental preparation. A single muscle fiber of 50–100 μm diameter and 3–5 mm long is hand-dissected and transferred to a custom-made double vaseline gap chamber filled with relaxing solution.

The bath chamber is similar to those used in other laboratories (Kovacs et al., 1983; Irving et al., 1987; Hui and Chen, 1992), but several adjustments have been made. The chamber is divided into three sections by two partitions. The width of each partition was changed from 300 to 100 μm. The middle section, called the central pool, has a width of 300 μm rather than 500 μm.

The isolated muscle fiber is mounted in the notches of the two partitions. The fiber is held in place, spanning the central pool, by two Delrin clips attached to the bottom of the two end pools using high vacuum grade stopcock grease. Tension is placed on the fibers to stretch the sarcomere to a length of 3–3.5 μm, measured under the microscope in each experiment. This step helps to keep the cell from contracting during the experiment. Thin vaseline seals and two glass cover slips are used to electrically isolate the three pools from each other. Six agar bridges connect the three pools to three small ponds filled with 3 M KCl. The agar bridges are glass tubes with inner diameter of 1 mm filled with agar gel made by normal Ringer's solution. The three intermediate ponds are connected to the electric circuit of voltage clamp through six Ag-AgCl pellets.

Pretreatment solutions

The muscle fiber segments in the two end pools were permeabilized using 0.01% saponin for 2 min. This treatment permits ionic conduction across the membrane. The saponin was then eliminated by washing out with relaxation solution and replaced with Cl^--free internal solution. In addition to the stretching of the fiber, 20 mM EGTA was added to the internal solution to further suppress contractions normally produced by electrical shocks. The central pool was filled with external solution containing Na and K channel blockers, tetrodotoxin, and tetraethylammonia (TEA) to eliminate voltage-gated Na and K channel currents. This adjustment was made after results of preliminary studies indicated that 1) the effects of neurotoxin binding on Na and K channels are not affected by electrical shock pulses, as shown in comparisons of blocking effects on the channel currents post-shock and pre-shock; and 2) the membrane potential threshold for damage to Na and K channels is much higher than the threshold for membrane electroporation. Damage to voltage-gated ionic channels by electrical shock will be discussed in a forthcoming paper.

Solutions

Contents of each of the solutions are described as follows. Relaxing solution contained 120 mM potassium glutamate, 1 mM $MgSO_4$, 0.1 mM K_2EGTA, and 5 mM K_2PIPES, pH 7.0. Internal solution contained 45.5 mM K.glutamate, 20 mM Tris-creatine phosphate, 20 mM K_2EGTA, 5.5 mM Na_2ATP, 5 mM glucose, 5 mM K_2PIPES, and 6.8 mM $MgSO_4$. External solution contained 120 mM TEA-Cl, 2.5 mM RbCl, 1.8 mM $CaCl_2$, 2.15 mM Na_2HPO_4, 0.85 mM $NaHPO_4$, and 1 μM tetrodotoxin, pH 7.1. TEA^+ and Rb^+ in the external solution were used to minimize K^+ currents and tetrodotoxin was for blocking Na^+ channels.

Voltage clamp configuration and its validity

This voltage clamp technique using double vaseline gap was developed by Hille and Campbell (1976) to study ionic channel currents and later adapted (Kovacs et al., 1983; Irving et al., 1987; Hui and Chen, 1992) to study charge movement. The voltage, *V1*, at the end pool 1 is monitored and compared with the command pulse. The difference between *V1* and the command pulse voltage is amplified and used to adjust the injecting current at the end pool 2 to keep *V1* within the prescribed command voltage. An advantage of this configuration is that the monitoring of membrane potential and the delivering of current occur in distinct pathways. Since no current passes though the voltage-monitoring pathway, the measured membrane potential at end pool 1 is not affected by the injected transmembrane current. However, because of the existing of the cell interior resistance, the voltage drop on these intracellular resistance results in a nonuniform membrane potential distribution in the central pool. This problem is important to consider in the study of electroporation on cell membrane, particularly when the high-voltage electrical shock pulse is delivered by voltage clamp.

First, during the rising phase of the shock pulse, the transient capacitance current of the cell membrane is significantly higher than the transmembrane current at steady state. This strong capacitance current results in a large voltage drop on the series intracellular resistance. To secure voltage *V1* at the end pool 1 as the command pulse voltage, the membrane potential along the rest of the fiber will experience a transient spike. The closer to the end pool 2, the higher is the spike overshock. This transient spike of the voltage at the end pool 2 may be many times higher than the magnitude of the shock pulse in the end pool 1.

We must note that this is a situation set up for a voltage clamp. It is different from the situation of an actual electrical injury, where transient capacitance current of the cell membrane slows down the building-up process of the membrane potential and there is never an overshock on the cell membrane. While the fiber is held by a voltage clamp, its membrane potential is constrained by the command pulse voltage in the end pool 1, no matter what changes occur in the cell membrane. The transient capacitance current cannot protect the cell membrane. Instead, the transient overshock voltage across the membrane resulting from the transient capacitance current may damage the cell membrane.

When we study electroporation by applying a high-voltage pulsed electrical shock on cell membrane, the cause of the membrane damage cannot be identified as either the magnitude of the shock pulse or the transient overshock voltage. It is difficulty to determine the membrane potential threshold of damaging and to study pulse-dependent damage of cell membrane. In fact, this transient overshock of the membrane potential also exists during measurements of the charge movement and the ionic channel currents using physiological range of command pulses.

Furthermore, because of intracellular resistance, the membrane potential in the central pool is not uniform even at steady state. According to cable theory, the intracellular membrane voltage distribution is an exponential decay along the axis of the cell from *V2* at end pool 2. The space constant is related to the membrane resistance of 1 cm^2 of membrane, R_m, and the intracellular resistance of 1 cm^3 of cytoplasm, R_i,

$$\lambda = (\rho R_m/2R_i)^{1/2} \quad (2)$$

where ρ represents the radius. For a healthy frog skeletal muscle fiber, the space constant is about 2 mm (Katz, 1966). We assume that the cell membrane resistance R_m of an electroporated muscle fiber is reduced a hundredfold, and therefore the membrane space constant of the eletroporated fiber is reduced by a factor of 10, resulting in a space constant of only 0.2 mm. If the central pool is 0.5 mm wide, the membrane potential at the border (next to end pool 1) of the central pool will only be 8% of the membrane potential at the border next to end pool 2. The ratio of the highest membrane potential over the lowest membrane potential in the central pool is 12.5. In other words, if the membrane potential at the end pool 1 is clamped at 300 mV, the membrane potential in the end pool 2 may be more than 3 V. If we also consider the intracellular resistance of the fiber segment at the area of the vaseline seal, the membrane potential in the end pool 2 is even higher. The schematic distribution of the membrane potential along the cell axis is shown as *curve A* at the *bottom* of Fig. 1.

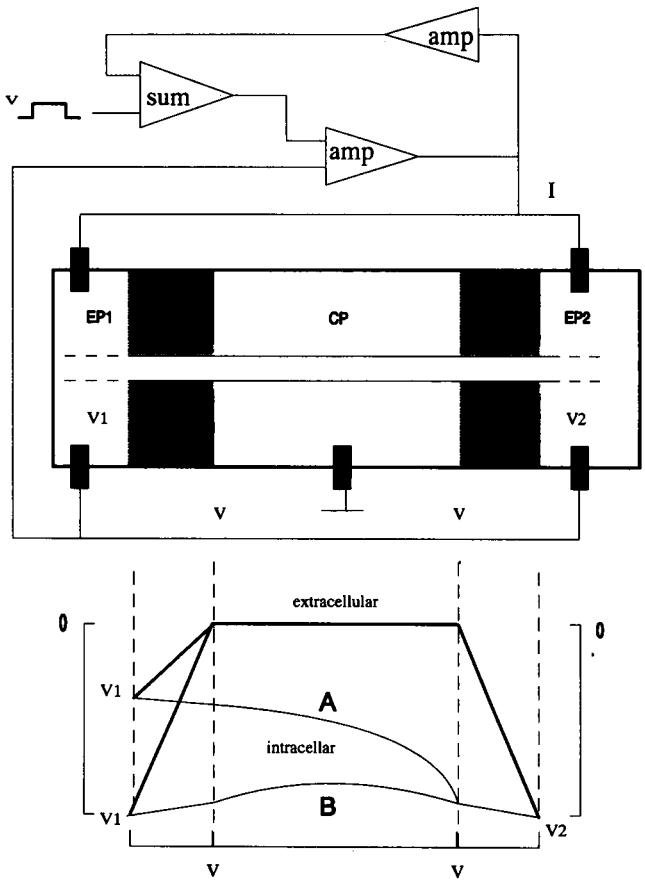

FIGURE 1 Schematic illustration of the new configuration of a voltage clamp with double vaseline gap chamber. At the *top* is the voltage clamp configuration. EP1, EP2, and CP represent end pools 1 and 2 and central pool, respectively. VS represents the vaseline seal partitioning the central and end pools. The central pool is connected to virtual ground to reduce noise and increase voltage clamping speed. End pools 1 and 2 are electrically connected. Voltage monitoring and current injection occur at both end pools 1 and 2. The injection current is split into the two end pools. The sensing signal of the total injection current is used to compensate for voltage dropped on the series intracellular resistance of the fiber at the segment beneath the vaseline seals. The membrane potential at the borders of the central pool should be the same as the command voltage. At the *bottom* are schematic drawings of membrane potential distribution along the axis of the fiber both for the traditional and the new configurations. The membrane potential outside the cell is represented by the dark lines; the membrane potential inside the cell is represented by the lighter lines. In the traditional configuration, the membrane potential in end pool 1 is held at the command voltage and the current is injected into the end pool 2. The membrane potential of the fiber decreases from point *V2* in end pool 2, linearly in the area of the vaseline seal, and then exponentially in the central pool, shown as *curve A*. In our new configuration, the membrane potential distribution is shown as *curve B* (see text). Both curves are drawn arbitrarily by eye.

The improved voltage clamp configuration with the double vaseline gap chamber is shown in Fig. 1 (*top*). Mainly, three aspects in our design differ from the traditional configuration. First of all, based on the above analysis of the space constant of muscle fiber, the size of the chamber was redesigned. The width of the central pool and each partition were reduced to 300 μm and 100 μm, respectively. These changes improve the membrane potential distribution in the central pool.

Second, end pool 1 and end pool 2 are electrically connected. The purpose of this change is to eliminate the transient overshock voltage on the cell membrane and to even out the distribution of the membrane potential

in the central pool. Now, both *V1* and *V2* in the two end pools are constrained by the command pulse, and no voltage spike exists during the pulses. The membrane potential distribution in the central pool was also been improved: 1) the injecting current is split into two pathways through both end pools 1 and 2 and through cell membrane to the central pool, so the equivalent fiber length is reduced by a factor of 2; 2) the equivalent cross-section of the fiber through which the injecting current passes is increased by 2. The new space constant on the cell membrane can be calculated by substituting these data in the Eq. 2. Using the same electroporated muscle fiber with the new clamp configuration and the new chamber, the ratio of the highest membrane potential to the lowest membrane potential in the central pool is only 1.8, seven times better than that obtained with the traditional configuration.

Finally, since the measurement of the membrane potential, V, and the current injecting, i, are in the same pools, the voltage drop of the injecting current on the series intracellular resistance of the fiber segment at the partition area will affect the accuracy in measurement of the membrane potential in the central pool. The measured membrane potential V, at end pools, is not the same as the membrane potential in the central pool. To overcome the voltage drop induced by the resistance of the interior of the cell, a series resistance compensation circuit has been developed as shown in Fig. 1. The injected current is fully monitored at the point of origin, and the signal is used to determine compensation voltage added to the command pulse. This extra voltage beyond the command pulse is used to compensate for the voltage drop of the transmembrane current on the series intracellular resistance at the partition. The transmembrane current varies during each pulse, and the positive feedback circuit can follow the changes in transmembrane current to compensate for voltage drops on the series intracellular resistance. The result is that the membrane potentials at the borders of the central pool close to the command voltage.

Electrical measurements

A voltage clamp from Dagon (Total Clamp 8800, Dagan Co., Minneapolis, MN) was used to control the transmembrane potential and simultaneously measure the amount of injected current. The central pool is connected as a virtual ground, V_0, to reduce noise and improve recording speed. The measurement circuit consists of a series of two parallel agar bridges with Ag-AgCl pellets.

The control commands are transmitted by a digital-to-analog converter (Data Translation DT 2825) from an IBM-compatible computer (Wells American 286, West Columbia, SC). The shape, magnitude and duration of the electrical pulses can be specified by the user from the computer keyboard. The transmembrane current was filtered at 3 kHz by an electronic filter (frequency device 902LPF) and then digitized by a digital oscilloscope (Tektronix 11401, Beaverton, OR). The digital oscilloscope interfaced with the computer through a general purpose interface bus board, (GPIB PCIIA). All traces, including voltage V and current I, were displayed on the oscilloscope screen, transmitted to the computer, and stored for future analysis. All experiments were performed at room temperature (24°C).

The Dagan Total Clamp 8800 has two voltage sources, 15 V and 100 V compliance. The measurement pulse is produced by the 15-V source, and the shock pulse is produced by the 100 V source. A head stage probe (Dagon 8866BP) is used to reduce noise and increase the ratio of signal to noise. When using a compliance-voltage source of 100 V, the model 8800 can provide at least 50 μA of current source, an amount that is enough to supply transmembrane current to an electroporated muscle fiber during a pulsed electrical shock.

The experimental protocol was as follows. When a single fiber was mounted into the chamber, central pool and end pools were filled with relaxing solution. At time 0, saponin treatment was applied to both end pools to permeabilize the cell membrane. After 2 min, the cell was rinsed using a relaxing solution for 3 min and then bathed in an internal solution. The relaxing solution in the central pool was replaced by the external solution. After 20 min, the chamber was mounted on a microscope (Nikon Microphot) and the voltage clamp was switched on. The resting potential was held at -90 mV. This is the reference voltage for all of the stimulation and shock pulses. The holding current varied from fiber to fiber with a range from 10 to 30 nA. Fibers were considered unstable and given up if the holding current was higher than 30 nA. In each experiment, there was a 30-min waiting period after the voltage clamp was switched on to allow ion diffusion in the cell to reach a steady state. Then a repeated 20-mV pulse was applied to the cell membrane to adjust the series resistance compensation of the cell interior resistance in the area of two vaseline partitions.

Two types of electrical pulses were used in these experiments: measurement stimulation pulses and electrical shock pulses. The magnitude of the measurement pulses was -40 mV and the duration was 40 ms. For the electrical shock, there was a pre-pulse of -20 mV magnitude and 4 ms duration applied to the cell membrane just before the application of each shock pulse. The responding current was used to estimate capacitance and normal leakage currents. The shock pulse had a fixed duration of 4 ms to mimic the real situation of electrical shock.

RESULTS AND DISCUSSION

The electroporated current studied in this paper is a pulse-induced transmembrane leakage current. The difference between electroporating leakage current on cell membrane and the protein-mediating current is that the latter is time-dependent and ionic-selective. To concentrate on the electroporated leakage current across the cell membrane and avoid any effects due to channel currents, all pulses used in these experiments, both measurement pulses and shock pulses, were negative, which hyperpolarized cell membrane. In addition, channel blockers were also used in the bathing solution to reduce the holding current by blocking the Na and K channels (possibly not necessary if only negative pulses are used).

Series resistance compensation

The procedure used to compensate series resistance was as follows. A -20-mV pulse was applied on the cell membrane repeatedly. The capacitive current transient evoked provided the information for properly compensating series resistance. We turned up the series resistance dial until a ringing or undershoot of the capacitance transient occurred. Trace B at the *top* of Fig. 2 shows the response current to a -20-mV step pulse recorded before the series resistance was compensated. After the compensation, *trace A* was recorded, which shows a larger magnitude of the spike and a shorter time constant. The percentage of compensation for the series resistance can be estimated by comparing the membrane capacitive transients before and after the compensation. When the series resistance dial was at 0 (*trace B*), the response membrane capacitive current showed a spike, I_c, with an exponential decaying to a steady-state plateau, I_∞. The membrane capacitance, C_m, can be calculated from the integral of the current transient divided by the voltage step -20 mV or from the following equation by fitting data to an exponential curve:

$$C_m = (\tau I_c)/\{V/[1 - (I_\infty/I_c)]\} \quad (3)$$

Two methods can be used to estimate the series resistance. The membrane step voltage, 20 mV divided by the spike, I_c, is the series resistance. Because of the filtering effect, the accuracy is very low. We used the second method. The series

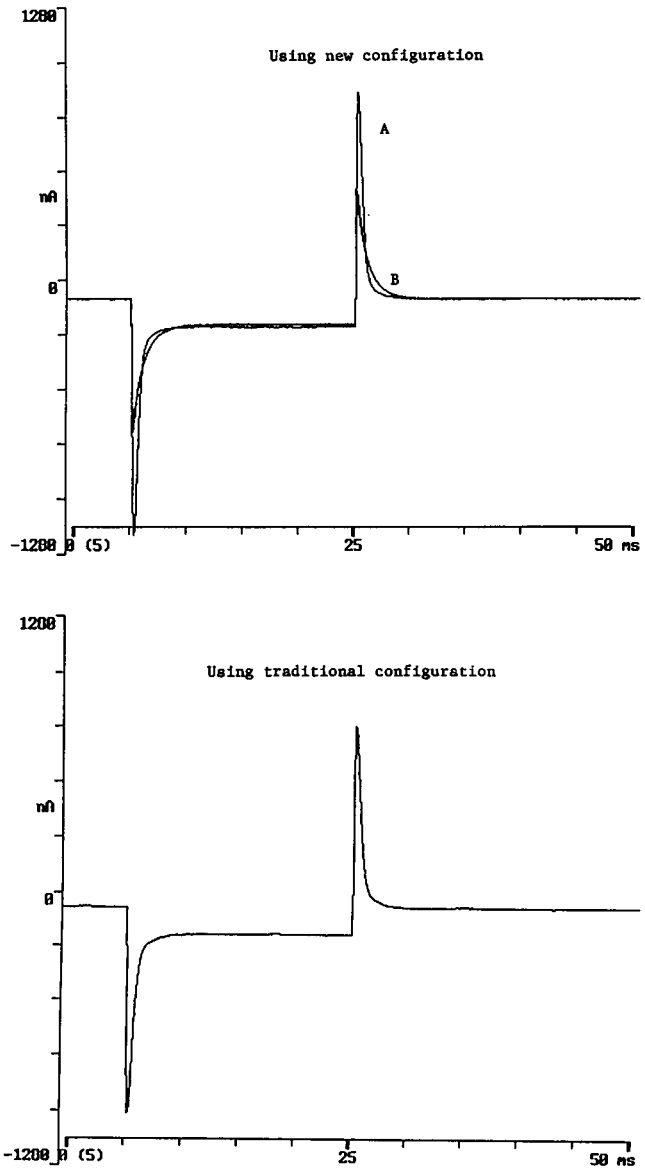

FIGURE 2 Comparison of the transmembrane current traces obtained before and after the series intracellular resistance compensation and the trace obtained by using the traditional configuration. Using the new configuration and the traditional chamber, the current *traces B* and *A* responding to a repeated 20-ms pulse of −20 mV were recorded before and after the compensation of the series resistance, respectively. Then, the configuration of the voltage clamp was changed to the traditional one and the gain of the amplifier was adjusted to the maximum value without oscillation. With the same chamber and the same stimulation pulse, the responding current was recorded and is shown at the *bottom*.

resistance is equal to the time constant, τ, of the exponential decay divided by the membrane capacitance. In our experiments, the ratio of the time constant τ_a/τ_b, where *a* and *b* represent after and before the compensation, is ~0.6–0.4. Approximately 40–60% of the total series resistance was compensated. Unlike the microelectrode, whole-cell voltage clamp, in which the series resistance source is the microelectrode, the source of a series resistance of a double vaseline gap voltage clamp is primarily from the interior of the cell, which includes two fiber segments (beneath vaseline and inside the central pool). The series resistance from the segment beneath the vaseline gaps is what we attempted to compensate. However, the segment inside the central pool also contributes to the series resistance. The segment beneath the vaseline gap is shorter, 100 μm, and its resistance has a constant weight factor that contributes to the exponentially decayed capacitive current, because all currents pass through this segment. The segment inside the central pool is longer, about half of the central pool, 150 μm, and its weight factors are gradually reduced from the border to the center of the central pool. No attempt was made in this study to accurately calculate the percentage of the total cell interior resistance attributed to the segment beneath vaseline gaps. The rough estimate is that less than half of the total series resistance can be attributed to the segment beneath the vaseline gaps. Then, at least 80–90% of the series resistance beneath the vaseline gaps was compensated. To compare the clamping speed using the traditional configuration and our configuration, a current response to the −20-mV step pulse was also recorded when using the traditional configuration and is shown at the *bottom* of Fig. 2. All of the situations were the same as those shown at the *top,* using the same traditional chamber. By comparing the transient magnitude of the responding currents, the current spike of *trace A* at the *top* is a little higher than the spike of the trace at the *bottom.* This result shows clearly that the clamping speed of our improved configuration was not reduced. Considering the fact that, using our small chamber, both membrane capacitance and cell interior resistance are reduced, the voltage clamping speed is improved.

Determination of shock pulse-induced leakage current beneath the vaseline seals

In the whole-cell voltage clamp, which uses a microelectrode, a gigaohm seal can form and leakage current is negligible. However, in the double vaseline gap voltage clamp technique, sealing is ineffective and current leakage is high. Chandler and Hui (1990) systematically studied the traditional double vaseline gap voltage clamp and concluded that most of the holding current resulted from the leakage current beneath the vaseline gaps. In our new chamber, the width of each of two partitions has been reduced to one-third of the traditional value to improve cell membrane potential distribution. Theoretically, the trade-off is that the sealing is reduced by one-third. In fact, with careful preparation, the holding current is similar to the holding current when the old chamber was used. In other words, the leakage currents beneath the vaseline seal must be removed and the transmembrane current has to be identified.

We note that the absolute value of the leakage current is not a problem and can be easily computationally removed by subtracting the template which can be obtained by scaling up the current response to a small pre-pulse. The question is how this leakage current beneath the vaseline seals relates to the stimulating pulse. If this leakage current is voltage-

independent, subtracting the pre-pulse template is a good method to identify the transmembrane current, even during a high voltage shock pulse.

One possible reason for the shock pulse-induced leakage is fiber-mechanical movement. Because of the presence of 20 mM EGTA and because the fiber stretches to a sarcomere of at least 3 μm, it is hardly surprising that the fiber, carefully watched under the microscope, did not twitch or contract during the shock. In fact, the holding current changed very little or not at all when the clips that held the fiber were occasionally moved, because vaseline is flexible and can adjust as the fiber moves. Another but less likely possibility is a electrical breakdown of the vaseline seal. Under voltage clamp, the potential differences across the cell membrane and across the vaseline seal are the same. However, the thickness of the cell membrane, about 50 Å, is several orders of magnitude lower than that of the vaseline sealing, 100 μm. The field strength across the cell membrane is 2×10^4 times higher than the field strength across the vaseline seal. Considering the similar hydrophobic and hydrophilic interactions that occur in cell membranes and in vaseline sealing, the field strength thresholds of electrical breakdown for these two should be similar. The shock pulse that can electroporate cell membrane should be far below the pulse that can break down the vaseline seals.

Experimentally, we designed two independent methods to prove our hypothesis. One is the measurement of the leakage current with ion-free isotonic solution in the end pools. The data in Fig. 3 show results from the second method. Fiber preparation was the same as that mentioned in Materials and Methods. The only difference was that voltage clamp was applied between the two end pools instead of between the center pool and end pools. A small pre-pulse of 20 mV followed by a shock pulse from 200–800 mV was delivered across the two end pools. The responding current consisted of two parts: one from the pathway through the interior of the cell between the two end pools and the other from the pathway beneath the two vaseline seals. The duration of saponin treatment of the fiber in the end pools was shortened to reduce the cell interior current so that it was comparable to the sealing leakage current. If the resistances through the two pathways are voltage-independent, the subtraction of the scaled pre-pulse response current from the shock pulse response should be 0. The traces in Fig. 3 were recorded during the shock pulses from 200 to 800 mV. The differences following subtraction of the templates obtained from the pre-pulses are shown as the bottom superimposed traces in the figure. The negligible remaining currents indicate that the vaseline seal is shock voltage-independent. Interestingly, the remaining current remains at 0 through the whole pulse duration, including the rising phase of the step function. This indicates that these seals are also not dependent on the rate of change of the voltage. These results agree with those obtained by using the ion-free isotonic solution and prove our hypothesis that leakage resistance beneath the vaseline seal is a voltage-independent constant.

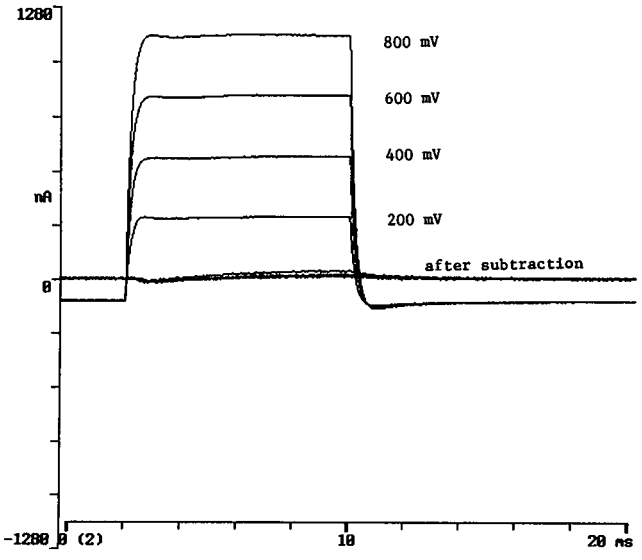

FIGURE 3 Measurements of the leakage currents beneath the vaseline seals. The voltage clamp was applied between the two end pools. The current traces were recorded responding to shock pulses 200, 400, 600, and 800 mV, as marked at the right column. After subtracting the response currents to small pre-pulses, respectively, the remaining currents are shown as the bottom traces.

Similar experiments with pre-pulse and shock pulse were also performed on the agar bridges and Ag-AgCl pellets, without a cell present and at different current densities. The same results were obtained, demonstrating that the resistance of agar bridges and the pellets is constant and voltage-independent, at least under the current density we used (up to 3000 nA). The resistance of the agar bridges and pellets was approximately 3 kΩ with either low or high pulses. At a transmembrane current of 2000 nA (typically electroporated membrane current during an electrical shock pulse of 600 mV), the voltage drop in the agar bridges and pellets was 6 mV, or 1% of the applied voltage.

Transmembrane current associated with a −40 mV measurement pulse before and after pulsed electrical shock

In Fig. 4 (*top*) is shown the stimulation pulse applied to the cell membrane. The transmembrane currents are shown at the *bottom*. The magnitude of the measurement pulse is −40 mV. *Trace A* in Fig. 4 was recorded before the shock. The sharp rise followed by exponential decay represents the charging current for membrane capacitance. Because the series intracellular resistance at the partition areas were compensated, the total apparent transmembrane resistance, R_m, is primarily determined by the steady-state transmembrane current, ΔI:

$$R_m = \Delta V/\Delta I \quad (4)$$

The steady-state transmembrane current, ΔI, responding to the stimulation pulse, can be obtained by subtracting the base line from the plateau of the current trace. The apparent membrane resistance includes membrane resistance plus cell interior resistance. In the theoretical analysis of the traditional

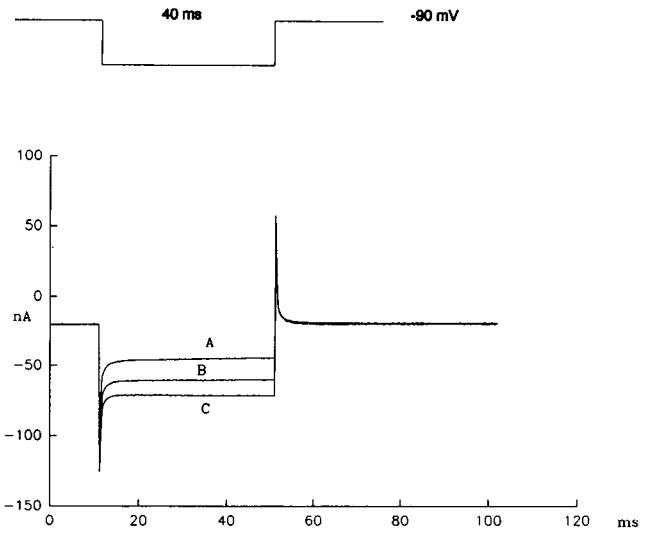

FIGURE 4 Measurement stimulation pulse and responding transmembrane currents. (*Top*) A stimulation pulse of −40 mV magnitude and 40 ms duration is applied on to the cell membrane before and after high voltage electrical shock. *Trace A* at the *bottom* shows the transmembrane currents responding to the stimulation pulse and taken as a control before the electrical shock. *Trace B* was taken after −500 mV, 4 ms electrical shock. The fiber was then relaxed at the resting potential for 10 min for full recovery. After another shock (−700 mV, 4 ms), *trace C* was recorded. The shock pulse-induced increment of the transmembrane current obtained from the plateau of each current trace indicates an increased membrane conductance associated with formation of electropores in the cell membrane.

configuration of double vaseline gap voltage clamp with *V1* and *V2* independent, Chandler and Hui (1990) found that the number of measurable parameters is not enough to solve the equation set without assumption that all hold current passing through vaseline seals. In the new configuration, *V1* and *V2* are the same, and it is more difficult to resolve membrane resistance analytically. The analytical resolution of specific membrane resistance is not the goal of this communication. However, attempts have been made to increase the ratio of the membrane resistance to the cell interior resistance in the apparent membrane resistance. Using the new configuration and redesigned chamber, the effective cell interior resistance is reduced to (about) 1/5 (150 μm/800 μm) of the interior resistance obtained in the traditional method. Because of the small size of the central pool in the new chamber, the membrane resistance is increased by a factor of 5/3 of that obtained with the traditional method. The ratio of the membrane resistance to the cell interior resistance is increased about eight times.

After the membrane was shocked by a −500 mV pulse of 4 ms duration, *trace B* responding to the same measurement pulse was taken and is shown at the *bottom* of Fig. 4. The steady-state transmembrane current, ΔI, increases. This result implies that the electrical pulse has destabilized the integrity structure of cell membrane, resulting in transmembrane leakage currents. After 10 min relaxation, the fiber was shocked again by a pulse of −700 mV and 4 ms duration. Then the same measurement pulse of −40 mV was applied to the membrane, and the responding transmembrane current was recorded and shown as *trace C* in Fig. 4. The rate of the increase in the steady-state transmembrane current depends on the magnitude of the shock pulse. Other experimental results show that the extent of electroporated membrane leakage current depends also on both the duration and the number of shock pulses.

A series of transmembrane current traces was also recorded for a sequence of −40 mV, 40-ms pulses with a interval of 1 min before and after electrical shock. The steady-state transmembrane currents obtained at the plateau were used as an indicator of the membrane leakage. Three traces were recorded before the shock and were averaged as a value of control. The transmembrane current responding to the first measurement pulse immediately applied after an electrical shock by a −500-mV pulse showed a significant increment of membrane leakage, which were up to as much as four times those taken before the shock. The series of current traces indicated that the membrane leakage slowly fell toward the control value with a time course of minutes. Fig. 5 plots the apparent membrane conductance, g_m, normalized to the value of the control, as a function of time before and after the electrical shock. The base line before the peak represents the current response to the −40 mV measurement pulse during the control period, i.e., before an electrical shock. A 4-ms shock pulse of −500 mV was applied at the fourth minute (Fig. 5). The first measurement pulse of −40 mV was given

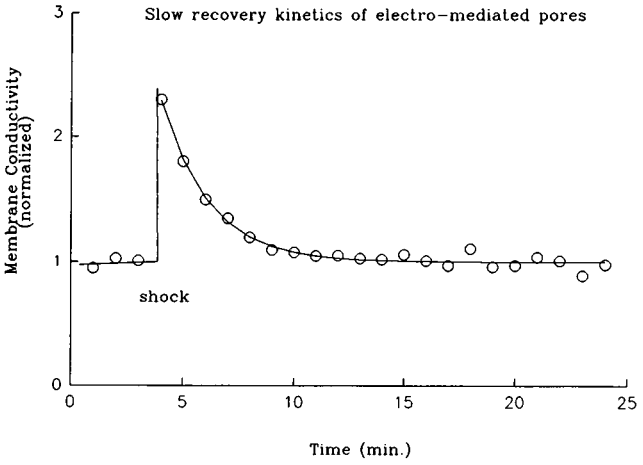

FIGURE 5 Transmembrane conductance versus time. Apparent membrane conductance was calculated from the steady-state transmembrane current following a sequence of measurement stimulation pulses of −40 mV, 4 ms. Data were normalized to a control value which is an average of the first three traces taken before the high electrical shock. A shock pulse of −500 mV magnitude and 4 ms duration was applied to the cell membrane at time of the fourth minute. Immediately (a few seconds) after the shock, the first transmembrane current trace was taken responding to the same measurement pulse. Then a sequence of the same measurement pulses were applied on the cell membrane with a interval of 1 min. The membrane conductance is dramatically increased by a high electrical shock and then slowly reduced to or close to the original value with a time course of about 5–10 min. The actual value of the membrane conductance varies with the diameter of the fiber. For this fiber, diameter was 70 μm, membrane conductance before the shock was 0.6 μS, and after shocked by a pulse of −500 mV of 4 ms duration was 1.6 μS.

immediately (a few seconds) after turning off the shock pulse, and the rest of measurement pulses were given in sequence every minute. The sudden peak in membrane conductance after the electrical shock indicates shock-induced ionic leakage, which implies a formation of electrically mediated pores or pore-like structures occurring in the cell membrane.

The slow monotonical decay of the membrane conductance toward the original value reveals that the membrane integrity structure is recoverable when the single shock pulse is −500 mV with 4 ms duration. This result suggests a spontaneous sealing process of reversible electroporation. The curve is obtained by fitting the data to an exponential decay. The best-fitting parameters for this fiber show that the time constant is 3.3 min. Seven fibers were used and the averaged best fitting time constant was 3.2 ± 0.8 min. This result indicates that self-sealing of the reversible electropores takes place in the cell membrane on a time scale of minutes. The time course to recovery was in good agreement with results obtained by measuring cytoplasmic free Mg^+ ion concentration and monitoring optical signals using a fluorescent dye, Mg-Fura-2, on mammalian skeletal muscle before and after electroporation (Canaday and Lee, 1990). Our results show that a strong electrical field can induce reversible leakage on the membrane of skeletal muscle cells, a conclusion consistent with the hypothesis that reversible electropores or pore-like structures can be induced by a strong electrical field on cell membranes (Tsong, 1991). The mechanism for this process is not yet clear. Further theoretical and experimental work is planned to define precisely these kinetics.

Effect of a −500 mV electric shock on cell membranes

The pulse shown in Fig. 6 (*top*) represents a 4-ms electric shock pulse of −500 mV across the muscle cell membrane. With a resting potential of −90 mV, the value of the membrane potential during the shock pulse is −590 mV. The trace shown at the *center* is the corresponding total transmembrane current recorded simultaneously during the pulsed shock. The transient jump with an exponential decay is capacitance current. The rising time of the capacitance charge current is constrained by the high-voltage compliance source in the voltage clamp. The transmembrane current then rises integrally throughout the pulse. This increasing current reflects the pulse-induced membrane leakage.

Compared with morphology studies of the shocked cell membrane using an electron microscope (Chang and Reese, 1990), the pulse-induced membrane leakage current is related to a formation of electromediated pores or pore-like structure in the cell membrane. Our experiments were designed to study the different components of electroporation on cell membranes and their time dependencies, including the time courses of formation and recovery of electropores occurred in cell membranes. To identify the pulse-induced leakage currents, the capacitance and normal leakage current have to be differentiated. The normal leakage and capacitance currents can be templated by scaling up the transmembrane current in response to the pre-pulse of −20 mV for 4 ms applied right before the shock. The pulse-induced electroporated current can be separated from the total transmembrane current by subtracting the template current, as shown at the *bottom* of Fig. 6. Meanwhile, the amount of the leakage current beneath the vaseline seal had been also subtracted as in the template. As mentioned previously, the leakage resistance beneath the vaseline seals, as well as the resistance of agar bridges and Ag-AgCl pellets, are constants and voltage-independent under our experimental situation. The remaining currents of subtraction are primarily pulse-induced transmembrane currents.

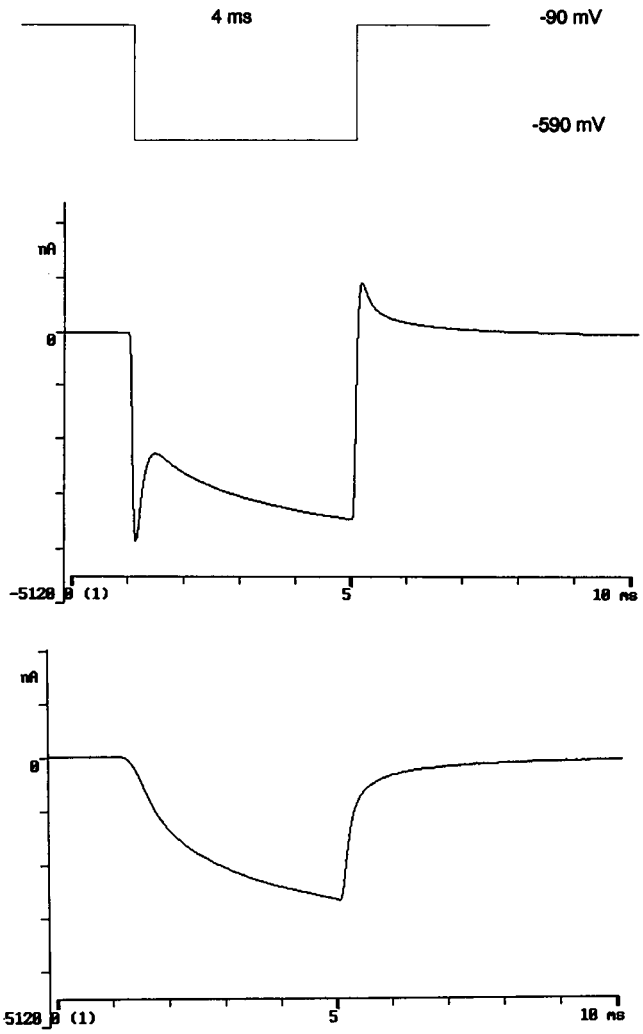

FIGURE 6 Transient transmembrane current recorded during a high electrical shock. The *top* shows a shock pulse of 4 ms duration and −500 mV magnitude. The *center* shows the recorded responses of transmembrane current to the shock pulse. After computationally removing the capacitance and the leakage currents of the normal cell membrane, as well as the leakage current beneath the vaseline seals by subtracting the template taken before the shock, the pulse-induced transmembrane current is differentiated and shown at the *bottom*. The pulse-induced leakage current depends on the magnitude and duration of the shock pulse and most of this leakage current reduces within milliseconds when the shock pulse is removed.

The electromediated current keep monotonically increasing until the end of the shock pulse, shown at the *bottom* of

Fig. 6. Starting from the falling edge of the electrical shock pulse, the pulse-induced leakage current decreases significantly within a millisecond and reaches a small and relatively stable plateau. Because this current is pure pulse-induced transmembrane leakage current, the off-time course should reflect the recovery process of the reversible membrane damage. This recovery time course is consistent with the results of other investigators (Tsong, 1991). Combining the recovery time constant obtained from the family of measurement pulses taken after the shock pulse (on an order of minutes; see Fig. 5) and the recovery time course of electropores obtained directly from the shock pulse (on an order of milliseconds; see Fig. 6), it appears either that two kinds of electropores simultaneously exist in a shocked cell membrane, at least with a difference of recovery time course of three orders of magnitude, or the electropores in the shocked cell membrane have two stages of recovery, one stage finishing in milliseconds and the second in minutes. Either way, the first and the secondary pores can be defined by the recovery time course. In the fast recovery time course, short-lived pores seal within milliseconds. In slow recovery time course, pores or pore-like structures may result from the secondary effect of an external high electrical pulse and seal within minutes. Our results do not rule out the possibility of electropores with other sealing time scales. Of interest is the fact that the short-lived pores contribute the most to membrane conductance, while the secondary pores contribute little.

CONCLUSION

The study of cell membrane electroporation has focused primarily on membrane transport of molecules, dyes, and genetic material. Few studies of electroporation have directly measured the electrical parameters of cell membranes, such as membrane potential, transmembrane current, and membrane conductance, particularly in large cells, such as skeletal muscle and nerve. The present study introduces an improved voltage clamp technique and a double vaseline gap chamber to study electroporation in frog skeletal muscle cells.

Simultaneous measurement of transmembrane potential and current makes it possible to calculate membrane conductance directly and resolve it into different components, as well as their time dependencies. The ability to record transmembrane current during the electrical shock significantly increases time resolution and facilitates the study of electrically mediated pores in cell membranes. With these new techniques we can better understand the mechanism of pores formation, reversible electrical breakdown, and rupture of cell membranes.

The work presented in this paper is the first application of the voltage clamp to measure transient transmembrane current during and after a strong electrical pulse in living skeletal muscle cells. The new voltage clamp configuration eliminates overshocking cell membrane and more evenly distributes membrane potential throughout the central pool. The positive feedback circuit makes it possible to measure more accurately membrane potential and to allow fast change of voltage on the cell membrane. The technique allows direct measurement of transmembrane current and solving into its components at a fixed constant transmembrane potentials. This, in turn, makes it possible to monitor functional changes of membrane proteins during and after a high voltage electrical shock, such as voltage-gated Na and K channel proteins on sarcolemma membrane and proteins of dihydropyridine receptors in the transverse tubular membrane of skeletal muscle cells. Because of more even membrane potential distribution and faster response to pulsed membrane potential change, this technique is also suitable for membrane study under physiological conditions.

We thank Drs. R. Dean Astumain and L. Tung for helpful comments, and Diane Rudall and Philip River for editorial assistance.
This work was supported by grants from Electric Power Research Institute, the Empire State Electric Energy Research Corporation.

REFERENCES

Abidor, I. G., V. B. Arakelyan, L. V. Chernomordik, Y. A. Chizmadzhev, V. F. Pastushenko, and M. R. Tarasevich. 1979. Electric breakdown of bilayer membranes. I. The main experimental facts and their qualitative significance. *Bioelectrochem. Bioenerg.* 6:37–52.

Benz, R., and U. Zimmerman. 1980. Relaxation studies on cell membranes and lipid bilayers in the high electric field range. *Bioelectrochem. Bioenerg.* 7:723–739.

Benz, R., and U. Zimmerman. 1981. The resealing process of lipid bilayers after reversible electrical breakdown. *Biochim. Biophys. Acta.* 640:169–178.

Canaday, D. J., and R. C. Lee. 1990. Magnesium ion flux measurement in skeletal muscle cell electroporation. *J. Cell Biol.* 111:431a. (Abstr.)

Chandler, W. K, and C. S. Hui. 1990. Membrane capacitance in frog cut twitch fibers mounted in double vaseline-gap chamber. *J. Gen. Physiol.* 96:225–256.

Chang, D. C., P. Q. Gao, and B. L. Maxwell. 1991. High efficiency gene transfection by electroporation using a radio-frequency electric field. *Biochim. Biophys. Acta.* 1992:153–160.

Chang, D. C., and T. S. Reese. 1990. Changes in membrane structure induced by electroporation as revealed by rapid-freezing electron microscopy. *Biophys. J.* 58:1–12.

Chen, W., and C. S. Hui. 1991. Differential blockage of charge movement components in frog cut twitch fibers by nifedipine. *J. Physiol.* 444:579–603.

Chen, W., P. Li, and R. C. Lee. 1992. Efficacy of non-ionic surfactants for sealing electropermeabilized skeletal muscle fibers. *Biophys. J.* 61: A422.

Chernomordik, L. V., S. I. Sukharev, I. G. Adidor, and Y. A. Chizmadzhev. 1983. Breakdown of lipid bilayer membranes in an electric field. *Biochim. Biophys. Acta.* 736:203–213.

Chernomordik, L. V., S. I. Sukharev, S. V. Popov, V. F. Pastushenko, A. V. Sokirko, I. G. Abidor, and Y. A. Chizmadzhev. 1987. The electrical breakdown of cell and lipid membranes: the similarity of phenomenologies. *Biochim. Biophys. Acta.* 902:360–373.

Cole, K. S. 1972. Membrane, Ions and Impulses. University of California Press, Berkeley. 569 pp.

Glaser, R. W., S. L. Leikin, L. V. Chernomordik, V. F. Pastushenko, and A. I. Sokirko. 1988. Reversible electrical breakdown of lipid bilayers: formation and evolution of pores. *Biochim. Biophys. Acta.* 940:275–287.

Hibino, M., M. Shigemori, H. Itoh, K. Nagayama, and K. Kinosita, Jr. 1991. Membrane conductance of an electroporated cell analyzed by submicrosecond imaging of transmembrane potential. *Biophys. J.* 59:209–220.

Hille, B., and D. T. Campbell. 1976. An improved vaseline gap voltage clamp for skeletal muscle fibers. *J. Gen. Physiol.* 67:265–293.

Hui, C. S., and W. Chen. 1992. Separation of Qβ and Qγ components in

frog cut twitch fibers with tetracaine. *J. Gen. Physiol.* 99:985–1016.

Irving, M., J. Maylie, N. L. Sizto, and W. K. Chandler. 1987. Intrinsic optical and passive electrical properties of cut frog twitch fibers. *J. Gen. Physiol.* 89:1–40.

Katz, B. 1966. Nerve, Muscle and Synapse. McGraw-Hill, Inc., New York. 73–75.

Kovacs, L., E. Rios, and M. F. Schneider, 1983. Measurement and modification of free calcium transients in frog skeletal muscle fibers by a metallochromic indicator dye. *J. Physiol. (Lond.).* 343:161–196.

Lee, R. C. 1990. Biophysical injury mechanisms in electrical shock victims. *Proc. IEEE Eng. Med. Biol. Soc. (Phila.).* 12:1502–1504.

Lee, R. C., L. P. River, F. S. Pan, J. Li, and R. L. Wollmann. 1992. Surfactant-induced sealing of electropermeabilized skeletal muscle membrane in vivo. *Proc. Natl. Acad. Sci. USA.* 89:4524–4528.

O'Neill, R. J, and L. Tung. 1991. Cell-attached patch clamp study of the electropermeabilization of amphibian cardiac cells. *Biophys. J.* 59:1028–1039.

Serpersu, E. H., and T. Y. Tsong. 1983. Stimulation of a ouabain-sensitive Rb^+ uptake in human erythrocytes with an external electric field. *J. Membr. Biol.* 74:191–201.

Teissie, J., and T. Y. Tsong. 1980. Evidence of voltage-induced channel opening in Na/K ATPase of human erythrocyte membrane. *J. Membr. Biol.* 55:133–140.

Tsong, T. Y. 1991. Electroporation of cell membrane. *Biophys. J.* 60:297–306.

Winegar, R. A., J. W. Phillips, J. H. Yongblom, and W. F. Morgan. 1989. Cell electroporation is a highly efficient method for introducing restriction endonuclease into cells. *Mutat. Res.* 225:49–53.

Wong, T. K., and E. Neumann. 1982. Electric field mediated gene transfer. *Biochem. Biophys. Res. Commun.* 107:584–587.

Zimmermann, U., J. Vienken, and G. Pilwat. 1980. Development of drug carrier systems: electric field induced effects in cell membranes. *J. Electroanal. Chem.* 116:553–574.